Hydrodynamic stability of the strip casting process

P. Plaschko
Departamento de Física, Universidad Autónoma Metropolitana Iztapalapa
09340 México, D.F., Mexico
e-mail: peterxanum.uam.mx

Recibido el 1 de junio de 1999; aceptado el 14 de junio de 2000

A thin slice of melt travels through a long zone which is cooled from below. Disturbances of this process are characterized by three disparate lengths: the solidification length L^*, the wave length λ^* and the depth of the slab δ^*_∞. Experimental observations show small-amplitude long waves with lengths ratios $\delta^*_\infty/L \ll \lambda^*/L^* \ll 1$. This means that the waves are too long to "perceive" the vertical variations in the melt. Thus we use a linear approach to study the stability of long one-dimensional shallow water waves. We found one mode that grows slightly under the influence of the decreasing depth of the melt. Its wavelength is about one order less than the cooling length. These theoretical predictions are in qualitative agreement with experimental observations.

Keywords: Hydrodynamic stability; two-phase flow; solidification

Una banda delgada de material fundido se mueve en una zona larga refrigerada en su parte inferior. Las perturbaciones de este proceso son caracterizadas por tres longitudes diferentes: la de la solidificación (L^*), la longitud de onda λ^* y el ancho de la banda δ^*_∞. Los experimentos indican ondas largas con amplitudes pequeñas y proporciones $\delta^*_\infty/L^* \ll \lambda^*/L^* \ll 1$. Esto significa que las ondas son demasiado largas para "percibir" las variaciones verticales en el material fundido. Por esto usamos una teoría lineal para estudiar la estabilidad de ondas largas en aguas poco profundas. Encontramos un modo que crece débilmente bajo la influencia de la profundidad decreciente del material fundido. Esta onda tiene una longitud de onda cerca de $L^*/10$. Estas prediciones teóricas estan cualitativamente en acuerdo con onservaciones experimentales.

Descriptores: Estabilidad hidrodinámica; flujo de dos fases; solidificación

PACS: 47.20.-k; 47.20.Hw

1. Introduction

The evolution of disturbances in films on horizontal and on inclined walls was subject of intensive investigation during the last decades. Horizontal films, open channel flow, falling films, the effect of moving boundaries in coastal waters were investigated [1–6]. Our study concerns a different class of flows where the variation of the boundaries is brought about by phase changes. We consider in particular the evolution of hydrodynamic disturbances in continuous solidification. The latter is of extraordinary importance in modern metallurgical engineering (see Schneider [7]). To simplify the problem we assume that there exists a solidification front instead of a "mushy" two-phase region. As the solidification layer grows the disturbances become influenced by the decreasing depth of the melt. This study is strongly motivated by results found in experimental work performed by the Voest Alpine Industrianlagenbau (VAI), which is the industrial partner of the Christian Doppler Laboratory (see also the acknowledgement). In Fig. 1 we give a sketch of the pilot plant installed in the laboratories of the VAI. Preliminary tests indicated long low-amplitude waves which form harmonically varying grooves in the solidified steal and thereby reduce the quality of the strip (Digruber *et al.* [8]). It should be kept in mind, however, that the experimental investigation of the strip casting process associated with temperatures of about 1000°K is extremely difficult and theoretical predictions are particularly valuable to understand and control the strip casting process.

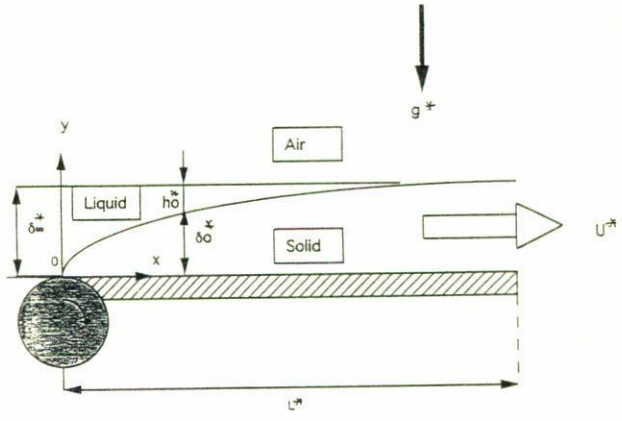

FIGURE 1. A sketch of the flow in the strip casting process.

The following analysis is based on the study of the linear stability of exact solutions to the Navier-Stokes equations. A particular feature of these solutions is that the mean flow is uniform. Thus we expect that the stability of the disturbances is mainly governed by geometrical effects like the growth of the solidified layer.

The investigation of Johnson [9] concentrates on the propagation of surface waves in irrotational flows over variable depth. By contrast, we have to consider here in addition to the variations of the depth the effects of the viscosity and of the convection of the material by the uniform speed.

2. Analysis

This study concerns the investigation of a horizontal strip casting process which takes place between a cooling table (length L^*) and a free surface. The melt is brought to the table via a conveyor roll (see Fig. 1). The roll is mounted such that its top defines the beginning of the cooling table and its velocity gives the uniform casting speed U^*. To produce a completely solidified melt the latter is cooled on the table from below. It is assumed that the constitution of the material excludes the formation of "mushy zones" and that segregation effects are negligibly. The solidification process takes place in the regime $0 \leq x^* \leq L^*$ and $0 \leq y^* \leq \delta^*_\infty$. We use variables with (without) an asterix to denote dimensional (non-dimensional) quantities. A slab of material moves at uniform speed (U^*). The melt flows in the uppermost layer and it and solidifies along the interface $y^* = \delta^*(x^*, t^*)$ and the solid is located in the lower regime $0 \leq y^* \leq \delta^*(x^*, t^*)$. We base the analysis on the assumption

$$\delta^*_\infty \ll \lambda^* \ll L^*. \tag{1}$$

Note that (1) represents a geometry which is typical for strip casting processes. The maximal thickness of the strip δ^*_∞ is assumed to be small relative to the wave length λ^*. This means that the waves are too long to "feel" the transverse structure of the layer. Hence we can apply one-dimensional (1D) flow equations. Note that 1D flow equations were also employed in [8]. The outer part of the inequality (1) implies that we may use a shallow water approach. Furthermore, we assume that the density of the material remains unchanged during the solidification process ($\rho^* = \text{constant}$).

The following basic equations are derived in the study of Kluwick and Scheichl [10]. They consist of 1D flow equations and 2D heat conduction equations

$$x = \frac{x^*}{L^*}; \quad y = \frac{y^*}{\delta^*_\infty}; \quad t = U^* \frac{t^*}{\lambda^*};$$

$$\delta = \frac{\delta^*}{\delta^*_\infty}; \quad h = \frac{h^*}{\delta^*_\infty}; \quad \varepsilon = \frac{\lambda^*}{L^*}; \tag{2}$$

$$u = \frac{u^*}{U^*}; \quad \theta_j = \frac{T^*_j - T^*_w}{T^*_s - T^*_w}, \quad j = 1, 2; \quad m = \frac{m^* \hat{L}^*}{\rho^* U^* \delta^*_\infty},$$

where u, θ_j, [the subscripts 1 (2) label upper (lower) layer] and m denote the velocity, temperatures and rate of solidification, respectively. T^*_s, T^*_w represent the temperatures of the solid and the of the wall. The hydrostatic pressure is given by (g^* is the gravity constant)

$$p^* = p^*_0 + \rho^* g^* (h^* + \delta^* - y^*). \tag{3}$$

Thus we obtain the 1D flow equations for the melt (momentum, continuity equation):

$$\left(\frac{1}{\varepsilon}\frac{\partial}{\partial t} + u\frac{\partial}{\partial x}\right) u + \frac{1}{F^2}\frac{\partial(h+\delta)}{\partial x} = \frac{2}{Re}\frac{\partial^2}{\partial x^2} u, \tag{4a}$$

$$\frac{1}{\varepsilon}\frac{\partial h}{\partial t} + \frac{\partial (hu)}{\partial x} + m = 0. \tag{4b}$$

Note that the viscous term on the right-hand side of (4a) is made up exclusively by normal stress terms. There are by definition no shear stresses in 1D flows. The energy equation has the form

$$\mathrm{Pe}_1 \left(\frac{1}{\varepsilon}\frac{\partial}{\partial t} + u\frac{\partial}{\partial x}\right) \theta_1 = \frac{\partial^2}{\partial y^2}\theta_1; \quad 0 \leq x \leq 1. \tag{4c}$$

Note that in our 1D approach there is no convective $v\partial/\partial y$ term in the energy equation. $\mathrm{Pe}_{1,2}$ labels the Péclet numbers, F, Re are Froude and Reynolds number, respectively. They are defined by

$$F = \frac{U^*}{(\delta^*_\infty g^*)^{1/2}}; \quad Re = \frac{U^* L^*}{v^*}. \tag{5}$$

The equations governing the dynamics of the solidified material are given by

$$u = 1; \quad \frac{1}{\varepsilon}\frac{\partial \delta}{\partial t} + \frac{\partial \delta}{\partial x} - m = 0, \tag{6a}$$

and

$$\mathrm{Pe}_2 \left(\frac{1}{\varepsilon}\frac{\partial}{\partial t} + \frac{\partial}{\partial x}\right) \theta_2 = \frac{\partial^2}{\partial y^2}\theta_2. \tag{6b}$$

The rate of solidification m is defined by ($A_{1,2}$ are the characteristic constants of mass transfer)

$$m = A_1 \frac{\partial \theta_1}{\partial y}(x,\, y = \delta) - A_2 \frac{\partial \theta_2}{\partial y}(x,\, y = \delta);$$

$$A_{1,2} = \text{const.} \tag{7}$$

The six equations (4) and (6) and (7) govern the six variables $u, h, \delta, \theta_{1,2}, m$. According to [8] and to Mörwald and Schneider [11], the exact steady solutions have the form (we refrain from listing the temperature profiles)

$$u_0 = 1; \quad \delta_0 = \sqrt{x} \quad \text{and} \quad h_0 = 1 - \sqrt{x}. \tag{8}$$

Equation (8) means that the steady flow velocity is uniform and equal to the casting speed. There arise problems from the particular form of h_0 in (8). The height becomes small as the end of the cooling table is reached. This causes non-uniformities and the expansions break down (see second part of (11) and note that this non-uniformity is not present in the expansion (14)). This is related to the fact that h_0 does not reach its limits for $x \to 0$ and $x \to 1$ asymptotically. Hence we restrict the variation of the horizontal evolution to the interval $0.1 \leq x \leq 0.9$.

In the following we will focus on disturbances of the steady state. First we note that in the absence of temperature fluctuations we have

$$\theta_j = \text{const.} \quad j = 1, 2;$$

$$\delta = \delta_0(x) = \sqrt{x};$$

$$m = m_0 = \frac{1}{2\sqrt{x}}. \tag{9}$$

Now we see that the two remaining quantities u and h are governed by (4a) and (4b) with m given by the last part of (9).

If we wish to include the case of temperature fluctuations we can use, however, a set of similar equations. We eliminate m from (4b) and (6a) and we obtain

$$\frac{1}{\varepsilon}\frac{\partial(h+\delta)}{\partial t}+\frac{\partial(\delta+hu)}{\partial x}=0. \tag{10}$$

Equations (4a) and (10) contain now the three quantities u, h and d. There seems to be a lack of one additional equation. We will see, however, in a moment that we can derive with the use of an asymptotic expansion a hierarchy of coupled equations where only u and $z=h+\delta$ are involved.

We introduce now an asymptotic expansion

$$\begin{aligned} u(x,t) &= 1+\Delta u_1+\Delta\varepsilon u_3+O(\Delta^2,\Delta\varepsilon^2),\\ h(x,t) &= h_0+\Delta h_1+\Delta\varepsilon h_3+O(\Delta^2,\Delta\varepsilon^2), \qquad (11)\\ \delta(x,t) &= \delta_0+\Delta\delta_1+\Delta\varepsilon\delta_3+O(\Delta^2,\Delta\varepsilon^2), \quad \Delta\ll\varepsilon. \end{aligned}$$

Δ is a formal parameter and the reason for using a double limit expansion will become clear in a moment. We use the coefficients

$$u_j=u_j(x_1,x_2,t)$$

and

$$\begin{aligned} z_j &= z_j(x_1,x_2,t)\\ &= h_j(x_1,x_2,t)+\delta_j(x_1,x_2,t); \quad j=1,3,\ldots \end{aligned} \tag{12}$$

and introduce two scaled variables ($\tilde{x}$ is a reference position)

$$x_1=\frac{x-\tilde{x}}{\varepsilon}, \quad x_2=x. \tag{13}$$

The expansion (11)–(13) is chosen such the slow variations in the fluids depth enter the problem in the shallow water equations before the nonlinearities come in. Note that because of $h_0(1)=0$ the domain of validity of the expansion (13) is limited to $0<x<1$. Note also that the variables h and δ enter (4a) and (10) only in form of the combinations $z=h+\delta$ and $uh+\delta$. Thus we see obtain with the use of (11)

$$\begin{aligned} z &= 1+\Delta z_1+\Delta\varepsilon z_3+\ldots,\\ uh+\delta &= 1+\Delta(z_1+h_0u_1)+\Delta\varepsilon(z_3+h_0u_3)+\ldots \end{aligned} \tag{14}$$

Equation (14) shows that only the pair of quantities u_j and z_j enters the equations. The set of the two original Eqs. (4a) and (10) is therefore sufficient to describe the problem up to order $\Delta\varepsilon$. Thus we see that the flow equations decouple from the energy equations also in the case of temperature fluctuations.

In the study of inviscid wave propagation [10] expansions corresponding to (7) failed because near $x=1$ [where $h_0(1)=0$ holds], leading order and correction terms are equal of magnitude $h_0\approx\varepsilon h_1$ for $x=1-O(\varepsilon)$. Equation (14) indicates, however, that in our problem no such failure of the expansions arises because near $x=1$ we have $uh+\delta=1+\Delta(z_1+u_1)+\Delta\varepsilon(z_3+u_3)+\ldots$.

We substitute (11)–(14) into (4a) and (10) and we have also to scale the Reynolds number. A consistent scaling, which allows for viscous effects in the leading order is (R is the scaled Reynolds number)

$$Re=\frac{2R}{\varepsilon}, \quad R=O(1). \tag{15}$$

The factor "2" in (15) was introduced for convenience. We derive now an hierarchy of equations and we obtain in leading order

$$\begin{aligned} Lu_1+\frac{1}{F^2}Dz_1-\frac{1}{R}D^2u_1 &= 0,\\ Lz_1+h_0(x_2)Du_1 &= 0;\\ D=\frac{\partial}{\partial x_1}, \qquad L &= D+\frac{\partial}{\partial t}. \end{aligned} \tag{16}$$

Note that the variable x_2 is in (16) only a parameter. Thus we can eliminate z_1 and this yields

$$\pounds u_1=0; \quad \pounds=L^2-\frac{h_0(x_2)}{F^2}D^2-\frac{1}{R}D^2L. \tag{17}$$

The first correction is governed by

$$\begin{aligned} Lu_3+\frac{1}{F^2}Dz_3-\frac{1}{R}D^2u_3 &= \mathrm{RHS}_1;\\ Lz_3+h_0(x_2)Du_3 &= \mathrm{RHS}_2 \end{aligned} \tag{18}$$

with the inhomogenities

$$\begin{aligned} \mathrm{RSH}_1 &= \frac{\partial}{\partial x_2}\left[\frac{2}{R}Du_1-\left(u_1+\frac{1}{F^2}z_1\right)\right];\\ \mathrm{RSH}_2 &= -\frac{\partial}{\partial x_2}\left[z_1+h_0(x_2)u_1\right]. \end{aligned} \tag{19}$$

If we anticipate the wave forms (22) and (23) we see that $\mathrm{RHS}_{1,2}$ represent secular terms. To avoid resonance we set

$$\mathrm{RSH}_1=\mathrm{RSH}_2=0. \tag{20}$$

Note that (20) is the 1D-leftover of the Fredholm's alternative. A simple integration yields the two equations

$$\begin{aligned} \frac{2}{R}Du_1-(u_1+\frac{1}{F^2}z_1) &= g_1(x_1,t);\\ z_1+h_0(x_2)u_1 &= g_2(x_1,t), \end{aligned} \tag{21}$$

where the functions $g_{1,2}$ are undetermined for the moment. To solve (17) we use the forms

$$\begin{aligned} u_1 &= A(x_2)\exp[i\Phi(x_1,t)];\\ z_1 &= B(x_2)\exp[i\Phi(x_1,t)]. \end{aligned} \tag{22}$$

The functions A and B in (22) represent amplitudes which are yet unknown. The complex phase function, however, is given by

$$\Phi(x_1,t)=\xi-\omega t; \qquad \xi=\frac{1}{\varepsilon}\int_{\tilde{x}}^{\tilde{x}+\varepsilon x_1}k(s)ds, \tag{23}$$

where ω labels a frequency (or Strouhal number) and k denotes the wave number. Note that forms of the type (22) and (23) have been used frequently in recent studies of spatial stability of weakly non-parallel flows (*cf.* Plaschko [12]). Because of the appearance of the fast variable ξ in (23) we may also consider (22) with (23) to be the leading order term of a WKB-expansion (see, *e.g.*, Bender and Orszag [13]).

The introduction of (22) into (17) yields now the eigenvalue equation

$$i(k-\omega)F^2\left[i(k-\omega)+\frac{k^2}{R}\right]+k^2h_0(x_2)=0. \tag{24}$$

Note that the PDE (17) is of second order w. r. t. the time-variable and of third order w. r. t. the spatial variable x, (24) is hence an equation quadratic in the frequecy ω and cubic in the wave number. Because of the x-dependence of the solutions to (24) we may consider this equation as the one of locally parallel disturbances. The disturbances grow (or decay) in the horizontal direction and we consider in the following only spatially excited (or damped) waves with $k=k_r+ik_i;\omega\in\mathrm{R}$ Because of the cubic nature of (24) we expect three different modes as solution of (24). We can also conclude from (24) that the F-dependence of the eigenvalues decrease gradually as x increases. In the appendix we will juxtapose the solutions of (24) with the ones of a 2D characteristic value equation derived in a forthcoming g paper.

To study the inviscid limit of the characteristic values we use the expansion

$$k=k_0+\frac{k_1}{R}+O(R^{-2}). \tag{25}$$

The substitution of (25) into (24) leads to

$$k_0=\frac{\omega}{1\pm\dfrac{h_0^{1/2}}{F}}$$

and

$$k_1=\frac{1}{2}\frac{iF^3\omega^2}{(F\pm h_0^{1/2})^3}. \tag{26}$$

Note that $h_0^{1/2}/F=h_0^*g^*/U*=1/F_{\mathrm{loc}}$ where F_{loc} is the local Froude number. Note also one solution of the cubic equation (24) is lost because of the singular nature of the expansion (25). The solution with the minus sign in (26) represents a solution with a hydraulic jump at $F=h_0^{1/2}$ which occurs for $F<1$. We will compare the solution with the plus sign with one of the numerical solutions in Fig. 4.

We define the phase speed of parallel modes by

$$c_{\mathrm{ph}}^{(p)}=\frac{1}{U^*}\frac{dx^*}{dt^*}=\frac{1}{\varepsilon}\frac{dx}{dt}, \tag{27}$$

and we obtain with (23) $\Phi=\mathrm{const.}$, $c_{\mathrm{ph}}^{(p)}=\omega/k_r$.

To complete the analysis we have to determine the amplitudes A and B in (22). To accomplish this we substitute (22) into (21) and solve the corresponding system by consistently using the forms

$$g_1(x_1,t)=C\exp[i\Phi(x_1,t)],$$
$$g_2(x_1,t)=E\exp[i\Phi(x_1,t)];\quad C,E=\mathrm{const.} \tag{28}$$

This leads to

$$A(x)=A(\tilde{x})\frac{\sigma(\tilde{x})}{\sigma(x)};$$
$$\sigma(x)=h_0(x)+\left[\frac{2ik(x)}{R}-1\right]F^2;$$
$$B(x)=B(\tilde{x})+h_0(\tilde{x})A(\tilde{x})-h_0(x)A(\tilde{x})\frac{\sigma(\tilde{x})}{\sigma(x)}. \tag{29}$$

Note that we have now reached the final phase of the calculations and we use the physical coordinate x again. We define the gain (or loss) G_{u_1} for the velocity fluctuations. This is given by the fluctuating amplitude referred to the initial point

$$G_{u_1}(x,\tilde{x})=\left|\frac{\sigma(\tilde{x})}{\sigma(x)}\right|\exp\left[-\frac{1}{\varepsilon}\int_{\tilde{x}}^{x}k_i(s)ds\right],$$
$$G_{u_1}(\tilde{x},\tilde{x})=1 \qquad \tilde{x}\le x\le 1;$$
$$G_{u_1}(x,1)=\frac{G_{u_1}(x,\tilde{x})}{G_{u_1}(1,\tilde{x})}. \tag{30}$$

The second part of (30) is useful if we want to change the reference point. The phase speed is given by

$$C_{\mathrm{ph}}(x)=\frac{\omega}{k_r+\varepsilon\dfrac{v'u-vu'}{u^2+v^2}};$$
$$u+iv=\frac{1}{\sigma};\qquad '=\frac{d}{dx}. \tag{31}$$

3. Numerical results and discussion

In technical realizations of the strip casting process R and F are order-one parameters. Our numerical evaluation was done for

$$0.25\le R\le 8;\quad 0.5\le F\le 4;\quad \omega=O(10^{-1}). \tag{32}$$

As mentioned earlier, we found three different modes. Two of the disturbances travel downstream, one runs upstream and all three modes are damped. Figures 2a and 2b reveal a graph of the eigenvalues of these three modes. The downstream traveling mode number one is the least damped (or almost neutral) disturbance, its parallel growth rate is multiplied by a factor 100 in Fig. 2b. This shows clearly that the two other modes (number two runs downstream, mode number three travels upstream) are very strongly damped and they are not observable in experiments. Hence we concentrate in the following exclusively on the evolution of mode number one.

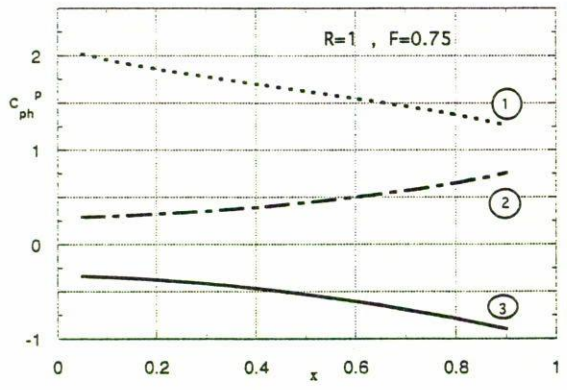

(a)

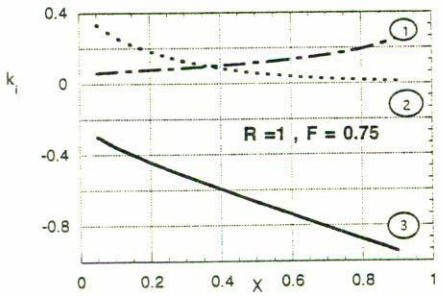

(b)

FIGURE 2. a) Parallel phase velocities of the three modes (mode one and two travel downstream, mode three runs upstream). $F = 0.75$, $\omega = 0.1$, $R = 1$; b) Like Fig. 2a) but parallel growth rates of the three modes. The growth rate of mode number one is multiplied by a factor 100.

The imaginary parts of the eigenvalues (or the parallel growth rates) of mode number one are revealed in Figs. 3 and 4. This quantity increases slightly during its horizontal evolution and becomes gradually F-independent as x increases. Figure 4 indicates the asymptotic tendency towards R-independence given by (25) and (26). The asympototic growth rates [caslculated with (26)] agree well at high values of the Reynolds number parametr R with growth rates calculated with (24). An increase of the Strouhal number (not shown in these figures) leads to an enhanced damping of the disturbances.

In Fig. 5 we present the numerical predictions of the gain and the local wave length λ_0^* of the disturbances. The latter quantity is with (29) and (31) given by

$$\frac{\lambda_0^*}{L^*} = \frac{2\pi\varepsilon c_{\rm ph}}{\omega}, \tag{33}$$

with $c_{\rm ph}$ given by (31). Thus we see that the disturbances are predicted to grow slightly in a first phase of the horizontal evolution and to decay later. The local wave length exhibits a maximum near the location of maximal gain and tends to a constant value for further downstream positions. These behavior—and the strong damping of the upstream traveling modes—can be ubderstood in terms of the wave energy. Downstream (upstream) traveling waves run into a layer of decreasing (increasing) depth and the conservation of wave energy leads thus to growth (decay). The final decay of the further is due to vicous damping.

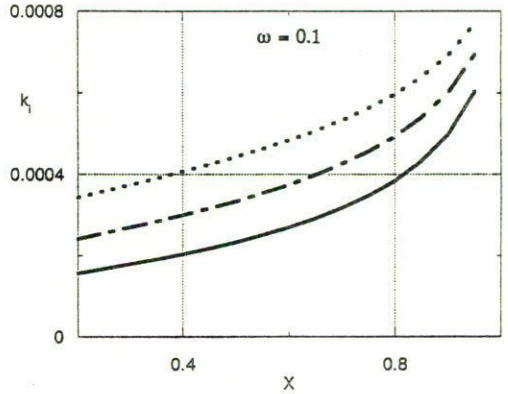

FIGURE 3. Parallel growth rates of mode one. Upper curve $F = 3$, middle curve $F = 1.5$, lower curve. $F = 0.75$, $\omega = 0.1$, $R = 5$.

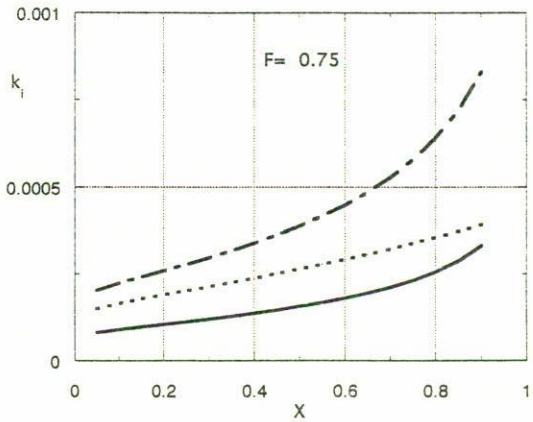

FIGURE 4. Like Fig. 3, but upper curve: $R = 3$, middle curve: asymptotic growth rate (26); lower curve: $R = 7.5$ $\omega = 0.1$, $F = 0.75$.

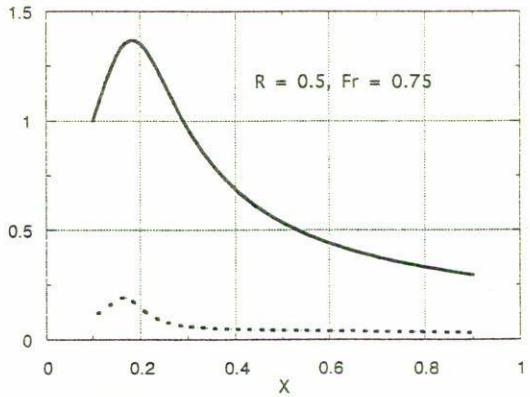

FIGURE 5. Gain (upper curve) and local wave length (lower curve) of mode number one. $R = 1$, $\omega = 0.1$, $F = 0.75$, $\varepsilon = 0.004$.

These predictions are in agreement with observations of harmonically varying small-amplitude grooves in the solidified material. The observed wave length has, however, a value of about $0.2 \leq \lambda_0^*/L^* \leq 0.3$. In contrast to the prediction of about $\lambda_0^*/L^* = 0.075$. The latter small value is nevertheless consistent with the assumption (1).

Acknowledgment

This research was initiated while the author was on sabbatical leave. He wishes to express his gratitude for partial support by the Christian Doppler Gesellschaft, Vienna, Austria. The author also gratefully acknowledges the access granted to preliminary experimental results obtained in a pilot plant at the Laboratories of the Voest Alpine Industrieanlagenbau, Linz, Austria. The authors dedicates this article to the memory of his friend, Professor Uwe Schaflinger, who died tragically April 2000.

Appendix

In a forthcoming paper [14] we will be publish a 2D approach to tackle the study of instabilities of the strip casting process. The corresponding eigenvalue equation is given by

$$\exp(\lambda\delta_0)[\lambda(\lambda^2 - r) + r\lambda\delta_0 - r] + \exp[\lambda(2 - \delta_0)] \times [\lambda(\lambda^2 - r) + r\lambda\delta_0 + r] = 0, \quad \text{(A.1)}$$

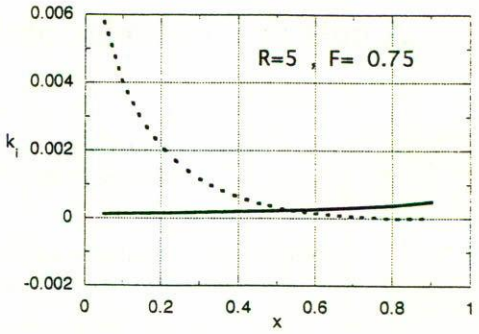

FIGURE 6. A comparison of 1D (continuous line) and 2D (dotted line) parallel growth rates, $R = 5, \omega = 0.1, F = 0.75$.

with

$$r = \frac{ikRF}{\left(1 - \frac{\omega}{k}\right)}; \quad \lambda^2 = iR(\omega - k); \quad \delta_0 = \sqrt{x}. \quad \text{(A.2)}$$

The corresponding eigenvalues are found to depend only rather weakly on the Weber number, the influence of which is not included in (A.1) and (A.2). In Fig. 6 we give now a comparison of the horizontal evolution of 1D (mode number one, governed by (24)) and 2D (governed by (A.1)) parallel growth rates. We obtain clearly the best agreement between the results of 1D and 2D approaches in an advanced regime of the horizontal development of the disturbances. There the slab is sufficiently thin to guarantee that the wave is much longer than the thickness of the molten material.

1. J. Lighthill, *Waves in Fluids*, (Cambridge University Press, Cambridge, 1977).
2. F.M. Henderson, *Open Channel Flow*, (Macmillan, New York, 1966).
3. A. Kluwick, *Acta Mechanica* **26** (1977) 15.
4. V.E.P. Nakoryakov, E.P. Pokusaev, and R. Schreiber, *Wave Propagation in Gas-Liquid Media*, (CRC Press, Moscow, 1993).
5. F. Engelund and O. Skovgaard, *J. Fluid Mech.* **52** (1973) 289.
6. J.R.L. Allen, P. Friend, A. Lloyd, and H. Wells, *Phil. Trans. R. Soc. Lond. A* **347** (1994) 291.
7. W. Schneider, *Arch. Eisenhüttenwesen* **54** (1983) 487.
8. M. Digruber, S. Haas, W. Schneider, and K. Moerwald, *Arch. Appl. Mech.* (1999), to be published.
9. R.S. Johnson, *J. Fluid Mech.* **276** (1994) 125.
10. A. Kluwick and S. Scheichl, *Phys. Fluids* **9** (1997) 3697.
11. K. Mörwald and W. Schneider, VAI-report Nr.93/24 (in German) (1993).
12. P. Plaschko, *J. Fluid Mech.* **92** (1979) 209.
13. C.M. Bender and S.A. Orszag, *Advanced Mathematical Methods for Scientists and Engineers*, (McGraw-Hill, New York, 1979).
14. P. Plaschko and U. Schaflinger, "Stability of two-dimensional strip casting processes", submitted to: *Phys. Fluids* (2000).